Protein farnesyltransferase in embryogenesis, adult homeostasis, and tumor development

Nieves Mijimolle,[1] Juan Velasco,[1,4] Pierre Dubus,[2] Carmen Guerra,[1] Carolyn A. Weinbaum,[3] Patrick J. Casey,[3] Victoria Campuzano,[1,5] and Mariano Barbacid[1,*]

[1]Molecular Oncology Program, Centro Nacional de Investigaciones Oncológicas (CNIO), E-28029 Madrid, Spain
[2]E.A. 2406, Histologie et Pathologie Moléculaire, University of Bordeaux-2, F-33076 Bordeaux, France
[3]Department of Pharmacology and Cancer Biology, Duke University Medical Center, Durham, North Carolina 27710
[4]Present address: Eli Lilly and Co., E-28108 Alcobendas, Madrid, Spain
[5]Present address: Departamento de Ciencias Experimentales y de la Salud, Universidad Pompeu Fabra, E-08003 Barcelona, Spain
*Correspondence: mbarbacid@cnio.es

Summary

Protein farnesyltransferase (FTase) is an enzyme responsible for posttranslational modification of proteins carrying a carboxy-terminal CaaX motif. Farnesylation allows substrates to interact with membranes and protein targets. Using gene-targeted mice, we report that FTase is essential for embryonic development, but dispensable for adult homeostasis. Six-month-old FTase-deficient mice display delayed wound healing and maturation defects in erythroid cells. Embryonic fibroblasts lacking FTase have a flat morphology and reduced motility and proliferation rates. Ablation of FTase in two *ras* oncogene-dependent tumor models has no significant consequences for tumor initiation. However, elimination of FTase during tumor progression had a limited but significant inhibitory effect. These results should help to better understand the role of protein farnesylation in normal tissues and in tumor development.

Introduction

Posttranslational modification of eukaryotic proteins by isoprenyl residues was firmly established in the late 80s (reviewed in Glomset et al., 1990; Zhang and Casey, 1996). Eukaryotic organisms, from yeast to man, contain three protein isoprenyltransferases, designated protein farnesyltransferase (FTase), protein geranylgeranyltransferase I (GGTase I), and protein geranylgeranyltransferase II (GGTase II). These enzymes are classified based on the isoprenyl group, farnesyl (C_{15}) or geranylgeranyl (C_{20}), that they use as a substrate as well as on the motif that they recognize. FTase and GGTase I (collectively known as CaaX prenyltransferases) recognize a CaaX motif where C is a cysteine residue, a is a small aliphatic amino acid, and X is the carboxy-terminal residue that contributes to substrate specificity. These enzymes are heterodimeric complexes comprised of a common regulatory (α subunit) and a unique catalytic (β subunit) subunit. In all cases, the isoprenyl group is attached to the protein by a thioether bond to the cysteine residue (Zhang and Casey, 1996).

Many substrates of CaaX prenyltransferases are involved in cellular pathways whose dysfunction often leads to disease. Among the best-known farnesylated proteins are Ras proteins, nuclear lamins, kinetochore proteins such as CENP-E and CENP-F, cGMP phosphodiesterase α, the γ subunits of two heterotrimeric G proteins, DnaJ heat shock protein homologs, rhodopsin kinase, and peroxisomal membrane proteins. GGTase I geranylgeranylates most of the members of the Rho subfamily of small GTPases, certain γ subunits of heterotrimeric G proteins, and cGMP phosphodiesterase α (Reid et al., 2004). Whereas FTase recognizes proteins with CaaX motifs in which X is a serine, methionine, alanine, or glutamine residue, GGTase I favors CaaX motifs in which the carboxy-terminal residue is a leucine (Seabra et al., 2002). However, enzyme specificity is not absolutely stringent, and there are abundant examples of protein crossprenylation (Zhang and Casey, 1996). For instance, K-Ras4B oncoproteins presumably escape functional inhibition by FTase inhibitors (FTIs) due to geranylgeranylation of its carboxy-terminal methionine by GGTase I (Lerner et al., 1997; Rowell et al., 1997; Whyte et al., 1997). Other proteins, such as RhoB, are substrates for both FTase and GGTase I (Armstrong et al., 1995). More importantly, farnesylated RhoB

SIGNIFICANCE

A significant number of proteins, including the Ras family, are isoprenylated, a posttranslational modification that is required for proper localization within membrane structures. Among isoprenylating enzymes, protein farnesyltransferase (FTase) has received most attention, since it can be targeted for pharmacological intervention to block transformation by Ras oncoproteins. Indeed, FTase inhibitors have been developed for over a decade and will be approved soon for clinical use. Here, we provide genetic evidence that FTase activity is essential for embryonic proliferation, but not for adult homeostasis. Surprisingly, FTase is not required for tumor induction by *ras* oncogenes. Yet, ablation of FTase during tumor progression results in significant tumor reduction. These findings should stimulate further work to better understand the role of protein farnesylation in cancer.

appears to have a different mechanism of action than its geranylgeranylated isoform (Du et al., 1999; Lebowitz et al., 1995), thus indicating that protein isoprenylation may confer distinct biological properties, at least to certain substrates (reviewed in Prendergast, 2001).

Among protein isoprenyltransferases, FTase has received special attention, since it is responsible for isoprenylating the Ras proteins implicated in a significant percentage of human cancers (reviewed in Downward, 2003; Sebti and Der, 2003). Early structure/function studies had indicated that replacement of the cysteine residue present in the CaaX motif of Ras oncoproteins by serine completely abolished their transforming activity in vitro (Willumsen et al., 1984a; Willumsen et al., 1984b). Later studies indicating that this cysteine residue was the site of modification by a farnesyl isoprenoid (Casey et al., 1989; Hancock et al., 1989) prompted the hypothesis that blocking farnesylation may have therapeutic benefit for cancer patients carrying *ras* oncogenes (reviewed in Gibbs et al., 1994). FTIs inhibited or delayed tumor development in human tumor xenografts (Kohl et al., 1994) and in H-*ras* transgenic models (Kohl et al., 1995) with few toxic effects. Several FTIs were rapidly taken to the clinic, and some of them are in phase III clinical trials (Downward, 2003). However, these compounds have not performed in the clinic to their initial expectations (Sebti and Der, 2003). Moreover, the mechanism by which FTIs induce antitumor effects remains to be elucidated, since their antitumor spectrum does not correlate with the presence of *ras* oncogenes (Sebti and Der, 2003).

We undertook this work to establish the genetic bases for the requirements of protein farnesylation in mammalian cells. To this end, we have generated constitutive (germline) and conditional (floxed) knockout strains of mice for the locus encoding the catalytic β subunit of FTase. We report here that protein farnesylation is essential for early embryonic proliferation but dispensable for postnatal development and adult homeostasis. Ablation of FTase in two *ras* oncogene-dependent tumor models has no significant consequences for tumor initiation. However, elimination of FTase during tumor progression had a limited but significant inhibitory effect. These observations have important implications, not only for understanding the biological significance of protein farnesylation in mammalian cells, but also in providing a much needed model for assessing the value of FTase as a target for cancer prevention and cancer therapy.

Results

Targeted disruption of the gene encoding the catalytic subunit of FTase

We have targeted the catalytic β subunit of FTase in embryonic stem (ES) cells by inserting three *loxP* sites flanking exon 3 and a PGK-*neo* cassette (*loxneo* allele) (Figure 1A). Removal of exon 3 causes a shift in the open reading frame leading to the incorporation of 26 unrelated residues before encountering a stop termination codon within exon 4 sequences. Crosses between $FT^{+/loxneo}$ and CMV-Cre transgenic mice (Schwenk et al., 1995) removed all floxed sequences to generate $FT^{+/-}$ heterozygous mice in 59 out of 62 newborn animals. In three mice, the Cre recombinase only removed the floxed PGK-*neo* cassette, thus generating the desired conditional allele (*lox* allele). The presence of the null (–) and conditional (*lox*) alleles was determined by Southern blot (data not shown) and PCR analysis (Figures 1B and 1C). Crosses between $FT^{+/-}$ mice failed to yield $FT^{-/-}$ animals. Crosses between $FT^{+/lox}$ mice resulted in the generation of $FT^{lox/lox}$ animals with the expected Mendelian ratio. These mice lived for over 2 years without obvious anatomical or behavioral abnormalities.

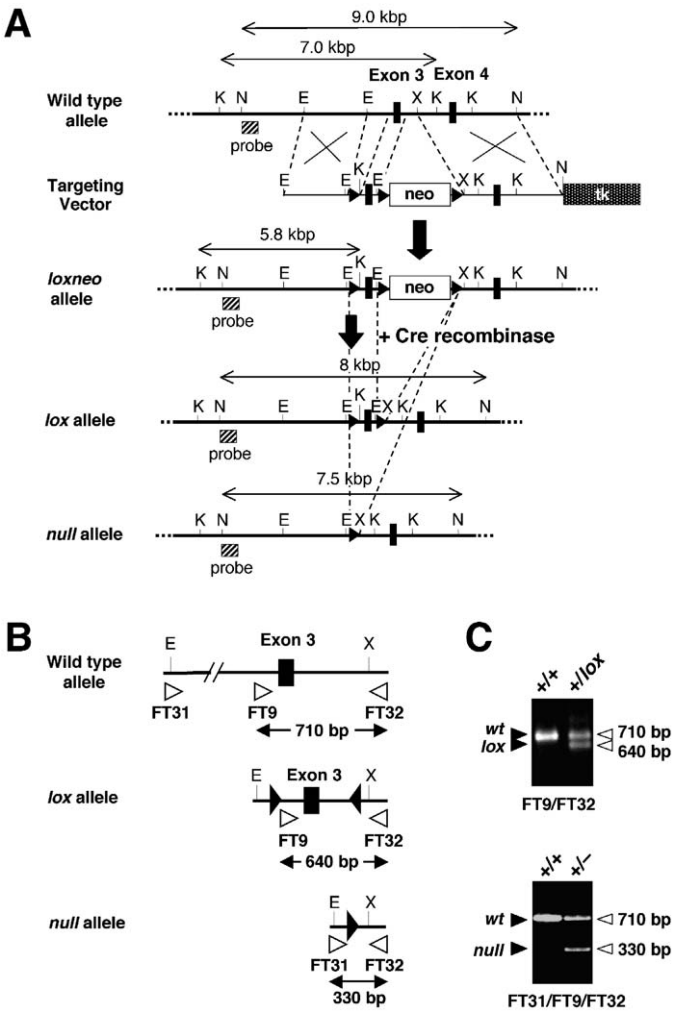

Figure 1. Gene targeting of the catalytic subunit of FTase

A: Genomic structure of the region encompassing exons 3 and 4 of the locus encoding the catalytic subunit of the mouse FTase. Those sequences included in the targeting vector are indicated by dotted lines. Exons 3 and 4 (filled boxes), PGK-*neo* cassette (open box), PGK-tk cassette (dotted box), and *loxP* sequences (filled triangles) are indicated. A homologous recombination event between the wild-type allele and the targeting vector yields the *loxneo* allele. The genomic structure of the conditional *lox* and null alleles resulting from partial and complete Cre-mediated recombination, respectively, of the *loxneo* allele is also indicated. The probe used to identify the diagnostic KpnI (K) and NheI (N) DNA fragments is indicated by a hatched box. Other diagnostic restriction sites, including EcoRI (E) and XbaI (X), are also indicated.

B: PCR strategy for routine genotyping. Forward (FT31, FT9) and reverse (FT32) primers are indicated by open triangles. The sizes of the expected diagnostic DNA fragments are also indicated.

C: Representative PCR analysis of tail DNA isolated from mice carrying the indicated alleles.

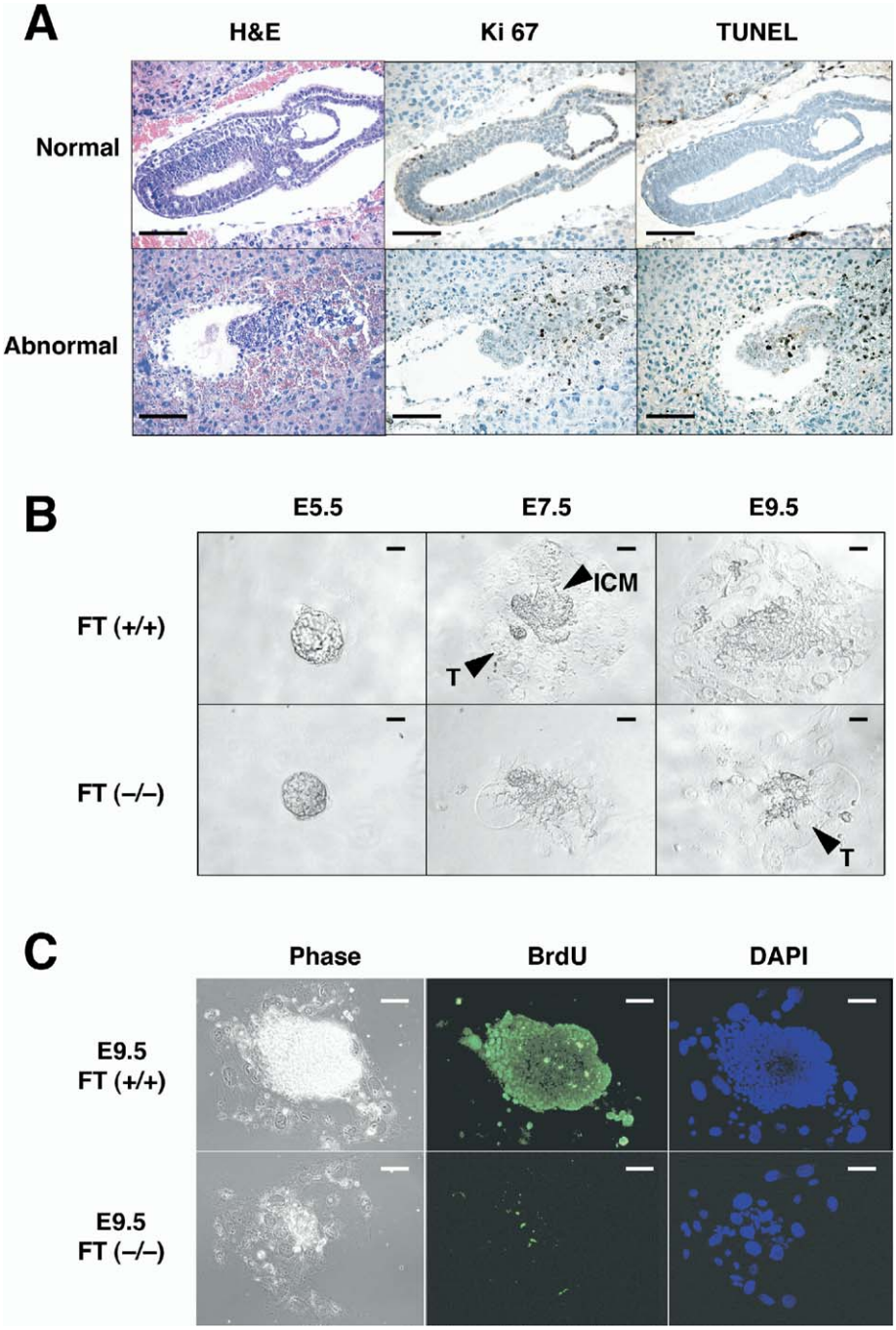

Figure 2. FTase is required for early embryonic development

A: H&E staining, Ki67 labeling, and TUNEL staining of representative sections from normal (top) and abnormal (bottom) E7.5 embryos derived from crosses between $FT^{+/-}$ mice. Abnormal embryos lacking detectable embryonic layers are likely to correspond to nonviable $FT^{-/-}$ embryos. The percentage of abnormal embryos coincided with the expected Mendelian ratio (25%) for $FT^{-/-}$ embryos. Normal embryos display high levels of Ki67-positive cells and no detectable apoptotic cells. In contrast, abnormal embryos have few Ki67-positive cells and multiple apoptotic cells.

B: Proliferative properties of $FT^{+/+}$ and $FT^{-/-}$ blastocysts in culture. Blastocysts (E3.5) derived from $FT^{+/-}$ crosses were placed on gelatin-coated plates and cultured for 2 (E5.5), 4 (E7.5), and 6 (E9.5) days. Cells were then used for genotype analysis. The inner cell mass (ICM) and trophoblast giant cells (T) are indicated.

C: Proliferative activity of $FT^{+/+}$ and $FT^{-/-}$ cultured blastocysts corresponding to E9.5 embryos as determined by BrdU incorporation. Phase contrast photographs (left) and DAPI staining (right) are also included. Scale bars, 100 μm in **A** and 4 μm in **B–C**.

FTase is essential for early embryonic development

Matings between $FT^{+/-}$ mice did not yield homozygous embryos at embryonic stage 11.5 (E11.5) or older. Histological examination of decidual swellings at E7.5 revealed a significant percentage of highly disorganized embryos with gross morphological alterations, including loss of the embryonic layers derived from the epiblast (Figure 2A). Only structures related to the ectoplacental cone and trophoblast giant cells could be morphologically identified. Loss of the epiblast in defective embryos appeared to be a consequence of decreased cell proliferation, as determined by a marked reduction of Ki67 immunostaining and increased apoptosis as revealed by high levels of TUNEL staining (Figure 2A).

To determine whether loss of FTase also had an effect on preimplantation embryos, we isolated E3.5 blastocysts from crosses between $FT^{+/-}$ mice. After 48–72 hr in culture, all blastocysts behave equally well in culture regardless of their genotype. They hatched and formed a multicomponent structure in which the inner cell mass (ICM) grew as a mound on top of the extraembryonic trophoblast cells (Figure 2B). However, after 4 days in culture, a stage equivalent to E7.5 embryos, the ICM of FTase null embryos showed a dramatic decrease in cell pro-

liferation (Figure 2B). These observations became even more evident 2 days later, when few $FT^{-/-}$ ICM cells persisted in the cultures and there was no detectable incorporation of bromodeoxyuridine (BrdU) (Figure 2C). In contrast, $FT^{-/-}$ trophoblasts remained attached to the culture dish and continued to grow in size at a rate similar to that of their wild-type counterparts, indicating that FTase may not be required for survival of endoreplicating cells (Figures 2B and 2C). These observations suggest that the defects observed in $FT^{-/-}$ embryos are an intrinsic property of the mutant embryonic cells.

Growth properties of FTase-deficient mouse embryonic fibroblasts

Due to the early lethality of $FT^{-/-}$ embryos, we used conditional FTase mutant mice to generate primary cultures of mouse embryonic fibroblasts (MEFs). First, we crossed $FT^{lox/lox}$ animals with $RERT^{ert/ert}$ mice, a strain that carries an IRES-CreERT2 cassette (Brocard et al., 1997) inserted by homologous recombination at the 3′ end of the locus encoding the large subunit of RNA polymerase II, between the terminator codon and the polyadenylation signal (*ert* allele). This strategy allows bicistronic expression of the inducible CreERT2 recombinase from the same mRNA as the large subunit of RNA polymerase II thanks to the knocked-in IRES sequences (our unpublished data).

Six independent cultures of $FT^{lox/lox};RERT^{ert/ert}$ MEFs derived from three different embryos were cultivated in the presence of 4-hydroxy-tamoxifen (4OHT), a synthetic steroid needed to activate CreERT2. Fully immortalized cultures were submitted to Southern blot analysis to determine whether the conditional *lox* allele had been completely excised. As illustrated in Figure 3A, all cultures contained varying amounts of null and *lox* alleles. To obtain a pure population of FT null MEFs, we isolated single-cell clones and submitted them to PCR analysis (Figure 3B). All 15 clones depicting an unambiguous $FT^{-/-};RERT^{ert/ert}$ genotype had a distinctly flat and polyhedric shape (Figure 3C). These FTase-deficient MEFs did not grow at high density and maintained a discernable intercellular space, a phenotype likely to result from cytoskeletal alterations. Indeed, the number of $FT^{-/-};RERT^{ert/ert}$ cells in saturated cultures was $1.48 \pm 0.79 \times 10^6$ per 10 cm dish (n = 3), whereas $FT^{lox/lox};RERT^{ert/ert}$ MEFs reached saturation levels that were three times higher ($4.50 \pm 0.12 \times 10^6$ per 10 cm dish; n = 3). These FTase-deficient MEFs also displayed reduced motility in an in vitro wound closure assay (Figure 3D).

FTase-deficient MEFs also proliferated less efficiently than control MEFs (Figure 3E) and had reduced plating efficiency. Whereas plating 5000 $FT^{-/-};RERT^{ert/ert}$ cells derived from three independent clones in a petri dish yielded 103 ± 7 colonies, the same amount of control $FT^{lox/lox};RERT^{ert/ert}$ MEFs led to 162 ± 3 colonies. Finally, quiescent $FT^{-/-};RERT^{ert/ert}$ MEFs reentered the cell cycle with normal kinetics upon serum stimulation (Figure 3F). However, the percentage of cells that entered S phase was reduced by about 60% when compared with that observed with $FT^{lox/lox};RERT^{ert/ert}$ MEFs (Figure 3F).

Absence of FTase activity in $FT^{-/-}$ MEFs

To date, the locus encoding the catalytic subunit of FTase appears to be unique within the human and mouse genomes. Yet, this fact does not preclude the existence of unrelated proteins with putative FTase activity. Thus, we examined whether

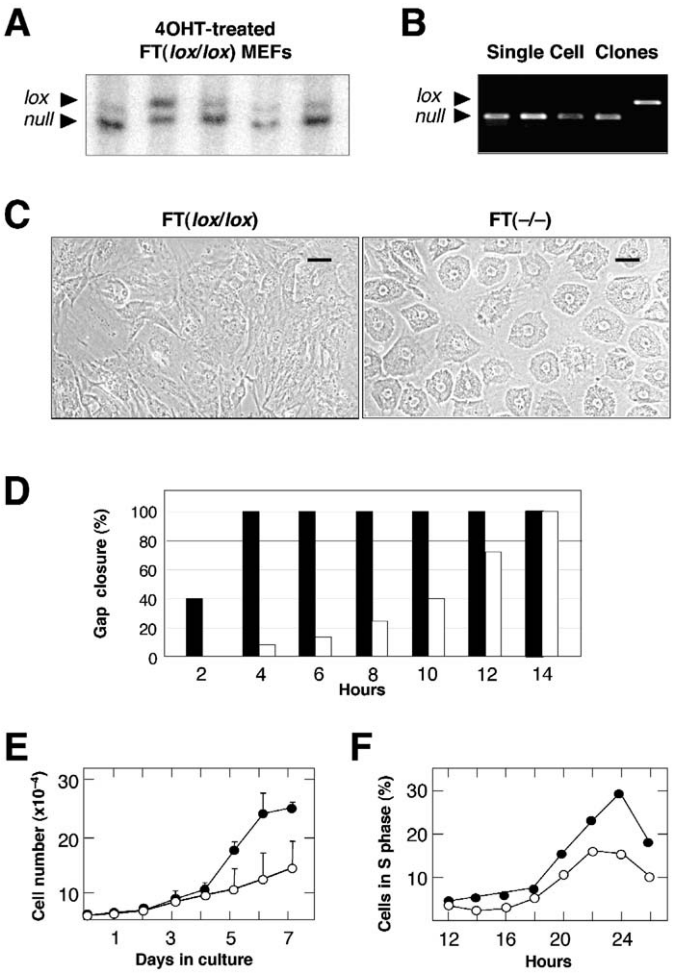

Figure 3. Growth properties of $FT^{-/-}$ MEFs

A: Southern blot analysis of individual cultures of passage 14 $FT^{lox/lox};RERT^{ert/ert}$ MEFs exposed to 4OHT.

B: PCR analysis of single-cell clones isolated from 4OHT-treated $FT^{lox/lox};RERT^{ert/ert}$ MEF cultures. Migration of the *lox* and null alleles is indicated by arrowheads.

C: Phase contrast photographs depicting the morphological appearance of MEFs expressing ($FT^{lox/lox};RERT^{ert/ert}$ MEFs) or lacking ($FT^{-/-};RERT^{ert/ert}$ MEFs) FTase. Scale bar, 8 μm.

D: Growth repopulation after mechanical injury in representative cultures of $FT^{lox/lox};RERT^{ert/ert}$ MEFs (filled bars) and $FT^{-/-};RERT^{ert/ert}$ MEFs (open bars). Results are represented as percentage of area filled at the indicated times.

E: Proliferation of immortal $FT^{lox/lox};RERT^{ert/ert}$ (filled circles) and $FT^{-/-};RERT^{ert/ert}$ (open circles) MEFs. Each time point was done in triplicate with three different cell lines of each genotype, and the average value is represented. At least three independent experiments were performed with all cell lines.

F: Kinetics of reentry in S phase upon serum stimulation of quiescent $FT^{lox/lox};RERT^{ert/ert}$ (filled circles) and $FT^{-/-};RERT^{ert/ert}$ (open circles) MEFs. In the description of the MEFs, the presence of the *ert* allele has been eliminated for clarity.

$FT^{-/-};RERT^{ert/ert}$ MEFs had detectable levels of FTase activity. Extracts derived from these cells failed to incorporate significant levels of ^{3}H-labeled farnesylpyrophosphate ([^{3}H]-FPP) into a biotin-labeled synthetic peptide substrate (biotin-YRASNRS-CAIM-COOH) derived from the carboxy-terminal sequences of human lamin B (Figure 4A). We also assayed FTase activity in

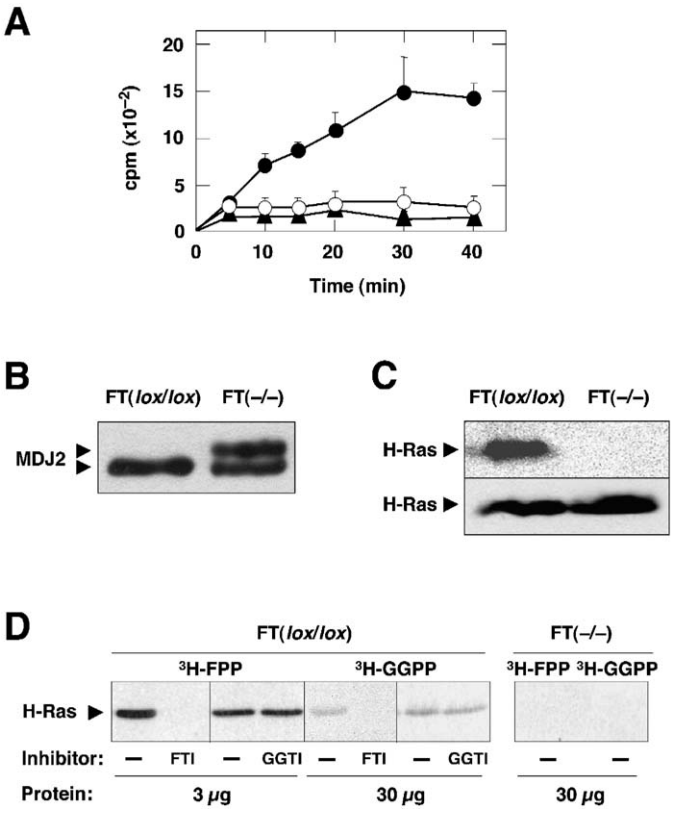

Figure 4. Lack of detectable FTase activity in $FT^{-/-};RERT^{ert/ert}$ MEFs

A: Extracts derived from $FT^{lox/lox};RERT^{ert/ert}$ MEFs either before (filled circles) or after (filled triangles) heat inactivation and from $FT^{-/-};RERT^{ert/ert}$ MEFs (open circles) were incubated with biotin-labeled lamin B peptide in the presence of [^{3}H]-FPP as described in the Experimental Procedures. The means ± SD for three different protein preparations are shown.

B: Electrophoretic analysis of MDJ2 in $FT^{lox/lox};RERT^{ert/ert}$ and $FT^{-/-};RERT^{ert/ert}$ MEFs. Migration of the MDJ2 protein isoforms is indicated.

C: (Top) Incorporation of [^{3}H]-FPP into H-Ras in extracts derived from $FT^{lox/lox};RERT^{ert/ert}$ and $FT^{-/-};RERT^{ert/ert}$ MEFs; (bottom) Western blot analysis of H-Ras immunoprecipitated from the same extracts.

D: Isoprenylation of recombinant H-Ras protein in vitro. Recombinant H-Ras protein was incubated with the indicated amount of cellular extract derived from $FT^{lox/lox};RERT^{ert/ert}$ or $FT^{-/-};RERT^{ert/ert}$ MEFs in the presence of [^{3}H]-FPP or [^{3}H]-GGPP. FTase (FTI) or GGTase (GGTI) inhibitors were added to the reactions as indicated. Migration of the H-Ras protein in SDS-PAGE gels is indicated by an arrowhead. All MEFs are homozygous for the *ert* allele.

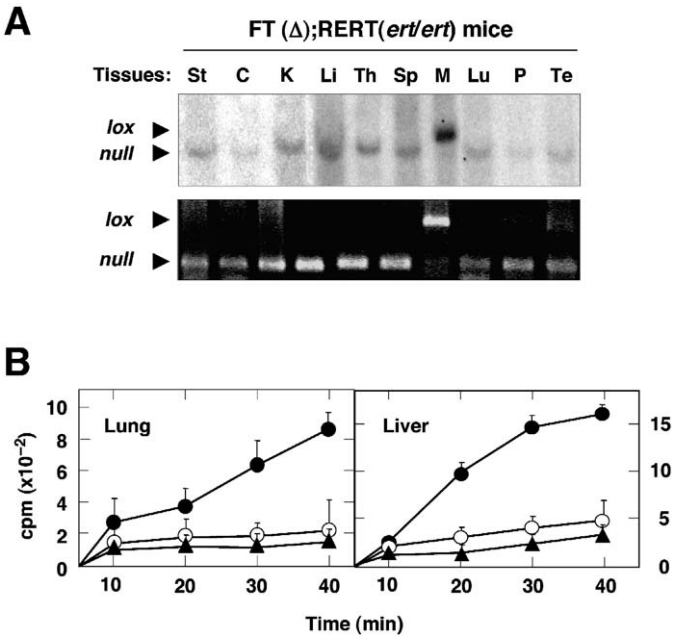

Figure 5. Lack of FTase in $FT^{-\Delta};RERT^{ert/ert}$ mice

A: Ablation of the gene encoding the catalytic β subunit of FTase in adult tissues. Southern blot (top) and PCR (bottom) analysis of DNA isolated from tissues of 2- and 4-month-old $FT^{-\Delta};RERT^{ert/ert}$ mice, respectively, generated by continuous treatment of P10 $FT^{lox/lox};RERT^{ert/ert}$ animals with 4OHT. The migration of the DNA fragments diagnostic of the *lox* and null alleles is indicated by arrowheads. Tissues included stomach (St), colon (C), kidney (K), liver (Li), thymus (Th), spleen (Sp), muscle (M), lung (Lu), pancreas (P), and testis (Te).

B: FTase activity in extracts derived from liver and lung tissues of $FT^{lox/lox};RERT^{ert/ert}$ mice before (filled circles) or after (filled triangles) heat inactivation and from $FT^{-\Delta};RERT^{ert/ert}$ mice (open circles). The means ± SD for protein preparations from three different animals are shown.

intact cells by determining the electrophoretic mobility of the endogenous MDJ2, a chaperone protein known to be a FTase substrate (Davis et al., 1998). As illustrated in Figure 4B, about 60% of MDJ2 expressed in $FT^{-/-};RERT^{ert/ert}$ cells displayed slower electrophoretic mobility likely to correspond to the non-farnesylated isoform. Whether the fast migrating MDJ2 present in FTase null cells is isoprenylated by GGTase I remains to be determined.

Next, we determined the ability of these FTase-deficient cells to farnesylate H-Ras. Total protein extracts from $FT^{lox/lox};RERT^{ert/ert}$ and $FT^{-/-};RERT^{ert/ert}$ cells were incubated with [^{3}H]-FPP followed by immunoprecipitation with anti-H-Ras antibodies. As illustrated in Figure 4C, only extracts from $FT^{lox/lox};RERT^{ert/ert}$ MEFs catalyzed the incorporation of [^{3}H]-farnesyl residues into H-Ras in spite of the presence of equal levels of H-Ras protein in both cell extracts. Finally, we performed a similar, albeit more sensitive assay using recombinant H-Ras protein. As depicted in Figure 4D, extracts from $FT^{-/-};RERT^{ert/ert}$ MEFs did not incorporate detectable [^{3}H]-FPP into recombinant H-Ras protein even under forced conditions (30 μg of protein) in which control extracts could even misincorporate ^{3}H-labeled geranylgeranylpyrophosphate ([^{3}H]-GGPP), as determined by using specific inhibitors (Figure 4C). Ablation of FTase activity has no effect on GGTase, since $FT^{-/-};RERT^{ert/ert}$ cells had normal levels of GGTase I activity (7.9 pmol/mg protein/hr). These results indicate that $FT^{-/-};RERT^{ert/ert}$ MEFs lack FTase activity.

Ablation of FTase in postnatal mouse tissues

Next, we examined the consequences of eliminating FTase during postnatal development. Ten-day-old (P10) $FT^{lox/lox};RERT^{ert/ert}$ or $FT^{lox/-};RERT^{ert/ert}$ mice were exposed to 4OHT for 8 weeks. At the end of treatment, FT *lox* alleles had been efficiently excised in all tissues except muscle (Figure 5A), a tissue in which the CreERT2 enzyme is not active in the RERT strain (V.C., unpublished data). Extracts derived from liver and lung tissues of 4OHT-treated animals had no significant levels of FTase activity (Figure 5B). These 4OHT-treated mice will be designated as $FT^{-\Delta};RERT^{ert/ert}$ regardless of whether they were

derived from $FT^{lox/lox};RERT^{ert/ert}$ or $FT^{lox/-};RERT^{ert/ert}$ animals, since we did not observe any differences between the two cohorts.

$FT^{\Delta};RERT^{ert/ert}$ mice did not display obvious anatomical, pathological, or behavioral defects for up to 18 months of age. Moreover, crosses between $FT^{\Delta};RERT^{ert/ert}$ males and wild-type females led to progenies in which more than 80% of the mice were $FT^{+/-};RERT^{+/ert}$, demonstrating that FTase null male germ cells are functional. The fertility of $FT^{\Delta};RERT^{ert/ert}$ females could not be assessed, since 4OHT treatment limits fertility even in wild-type females. Histological analysis of a variety of tissues of 2- to 3-month-old $FT^{\Delta};RERT^{ert/ert}$ mice, including bone marrow, colon, heart, kidney, liver, lung, lymph nodes, mammary glands, pancreas, pituitary gland, salivary glands, skin, spleen, stomach, testis, and thymus, did not reveal obvious histopathological alterations.

Stress responses in young mice lacking FTase

To test whether FTase was required during stress conditions, 10-week-old $FT^{\Delta};RERT^{ert/ert}$ mice were submitted to partial hepatectomy, wound healing, and erythropoietic regeneration after severe bleeding. Livers (about 70% of total tissue) were surgically removed from $FT^{lox/lox};RERT^{ert/ert}$ and $FT^{\Delta};RERT^{ert/ert}$ mice (n = 6). Nine days later, mice were sacrificed, and their livers were weighed. All animals displayed fully regenerated livers with no obvious morphological or anatomical differences between the untreated and the 4OHT-treated cohorts. Whereas $FT^{lox/lox};RERT^{ert/ert}$ livers weighed 2.15 ± 0.35 g, $FT^{\Delta};RERT^{ert/ert}$ livers had a weight of 2.40 ± 0.60 g. Genotype analysis of the regenerated liver tissue exclusively revealed the presence of the FT null allele (data not shown). $FT^{\Delta};RERT^{ert/ert}$ mice also recovered normally from skin wounds in the mid-dorsal region and from severe bleeding (data not shown).

Delayed wound healing in adult FTase-deficient mice

Six-month-old $FT^{\Delta};RERT^{ert/ert}$ mice were submitted to the same stress conditions except for partial hepatectomy, since at this age even wild-type mice have drastically reduced capacity to regenerate liver tissue. In the wound healing paradigm, we did not observe significant differences in the gross appearance of the wounds of $FT^{lox/lox};RERT^{ert/ert}$ and $FT^{\Delta};RERT^{ert/ert}$ mice (n = 12) 3 days after the incision. By day 5, all wounds were covered with a dry scab. All wounds were healed by day 9 in control mice. At this time, however, only 70% of the wounds in $FT^{\Delta};RERT^{ert/ert}$ mice had healed. Complete wound healing in these FTase-defective mice could not be observed until 12 days after incision. These observations indicate that $FT^{\Delta};RERT^{ert/ert}$ mice retain their full capacity to heal skin wounds. However, the regeneration process in these FTase-deficient animals is delayed by about 30%.

Maturation defects in erythroid cells of adult FTase-deficient mice

Morphologic examination of 6-month-old $FT^{\Delta};RERT^{ert/ert}$ mice revealed a minor but consistent decrease (about 20%) in the size of their spleens. Moreover, FTase-defective spleens had a significantly larger pool of proliferating Ter119$^+$ erythroid cells (7.7% ± 1.7% of total spleen cells versus 1.8% ± 0.5% in control mice) (Figure 6A). $FT^{\Delta};RERT^{ert/ert}$ spleens also had increased pools of myeloid cells compared to those of 4OHT-treated $FT^{+/+};RERT^{ert/ert}$ mice, including GR1$^+$ (22.77% ± 5.93% versus 10.45% ± 2.56% of Ter119$^-$ cells) and CD11b$^+$ (26.81% ± 1.5% versus 13.87% ± 0.45% of Ter119$^-$ cells) cells (Figure 6B). Whether the observed increase in myeloid cells is a direct consequence of FTase loss or an indirect effect caused by compromised erythroid maturation remains to be determined.

Removal of 0.8 ml of blood from 6-month-old 4OHT-treated $FT^{+/+};RERT^{ert/ert}$ and $FT^{\Delta};RERT^{ert/ert}$ animals (n = 6) resulted in a significant increase in the size of their spleens after 48 hr. This increase was more pronounced in wild-type mice (from 142 ± 7 to 245 ± 2 mg, 72% increase) than in those mice lack-

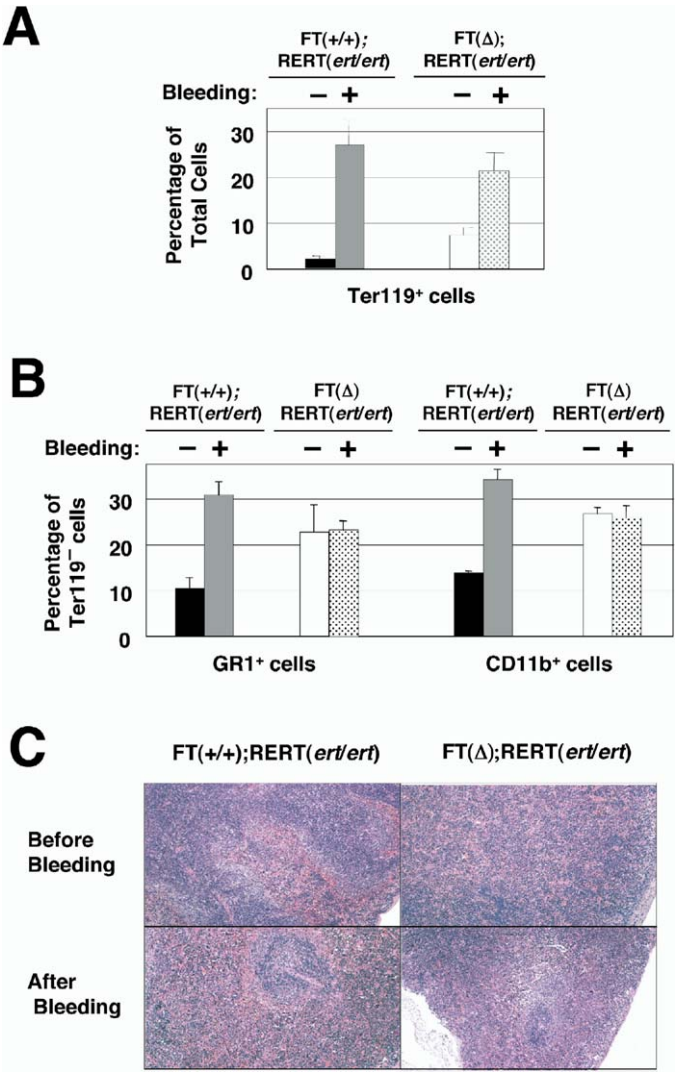

Figure 6. Erythroid defects in adult FTase mutant mice

A and B: Levels of splenic Ter119$^+$ erythroid (**A**) and GR1$^+$ and CD11b$^+$ (**B**) myeloid cells of 4OHT-treated $FT^{+/+};RERT^{ert/ert}$ and $FT^{\Delta};RERT^{ert/ert}$ 6-month-old mice before (−) and 48 hr after (+) removal of 0.8 ml of blood. The means ± SD for three different animals from each genotype are shown.

C: H&E-stained sections of the spleens depicted in **A** and **B** (original magnification 100×).

ing FTase (from 113 ± 4 to 175 ± 26 mg, 54% increase). Histological examination of these spleens revealed a significant depletion of reactive splenic erythropoietic centers in FT^{Δ};$RERT^{ert/ert}$ but not in $FT^{+/+}$;$RERT^{ert/ert}$ mice (Figure 6C). No differences were observed in the white pulp. Flow cytometry analysis indicated that, upon bleeding, the splenic erythroid compartment (Ter119$^+$ cells) of 4OHT-treated $FT^{+/+}$;$RERT^{ert/ert}$ mice increased by as much as 15-fold, whereas that of FT^{Δ};$RERT^{ert/ert}$ animals only increased by 2.8-fold (Figure 6A). We also observed different responses in myeloid cells. Whereas the number of GR1$^+$ and CD11b$^+$ cells increased by 2.5- to 3-fold in the spleens of 4OHT-treated $FT^{+/+}$;$RERT^{ert/ert}$ mice, no such increase could be observed in FTase-defective animals (Figure 6B). No differences were observed in Ter119$^+$, GR1$^+$, and CD11b$^+$ cells in bone marrow and peripheral blood before or after bleeding.

Ablation of FTase in tumors harboring K-*ras* oncogenes

To assess whether loss of FTase activity had an effect on tumor development, we ablated FTase in mice carrying lung adenocarcinomas induced by an endogenous K-*ras* oncogene (Guerra et al., 2003). To this end, we crossed $FT^{lox/lox}$;$RERT^{ert/ert}$ animals with $K\text{-}ras^{+/V12}$ mice, a strain that carries a conditional K-*ras* allele activated by a G12V mutation (Guerra et al., 2003). P10 $FT^{lox/lox}$;$K\text{-}ras^{+/V12}$;$RERT^{ert/ert}$ and $FT^{+/+}$;$K\text{-}ras^{+/V12}$;$RERT^{ert/ert}$ mice (n = 18) were treated with 4OHT for 24 weeks. Both cohorts developed multiple lung adenomas and adenocarcinomas at about 7 months of age (Guerra et al., 2003). As illustrated in Figure 7A, the number and size of adenomas present in both groups of mice were similar. Moreover, the percentage of adenomas that had progressed to adenocarcinomas at the time of death was also similar in both cohorts (22% in control mice versus 20% in FTase-deficient animals).

Other pathologies observed in 4OHT-treated $FT^{+/+}$;$K\text{-}ras^{+/V12}$;$RERT^{ert/ert}$ mice, including occasional facial and anal papillomas as well as hyperplasia in the Harderian glands, were also observed in FT^{Δ};$K\text{-}ras^{+/V12}$;$RERT^{ert/ert}$ animals with similar incidence (Figure 7B). Complete loss of FTase sequences in tumors isolated from FT^{Δ};$K\text{-}ras^{+/V12}$;$RERT^{ert/ert}$ mice was verified by PCR analysis (data not shown). These results indicate that K-*ras* oncogenes induce neoplastic lesions regardless of the presence or absence of FTase.

Loss of FTase does not prevent activation of H-*ras* oncogenes in carcinogen-induced tumors

Previous observations indicate that K-Ras oncoproteins can be crossprenylated by GGTase I in cells treated with FTIs (Lerner et al., 1997; Rowell et al., 1997; Whyte et al., 1997). Whether crossprenylation is responsible for the lack of effect of eliminating FTase in K-*ras*-induced tumors remains to be determined. In contrast, H-Ras cannot be isoprenylated by GGTase I (James et al., 1995) (Figure 4D). Therefore, we examined the requirement of FTase for H-*ras*-induced oncogenesis in vivo. To this end, we submitted FTase-defective mice to the classical 7,12 dimethyl-benzanthracene (DMBA) plus 12-*o*-tetradecanoylphorbol-13-acetate (TPA) skin carcinogenesis protocol in which H-*ras* oncogenes are frequently activated (Balmain and Pragnell, 1983).

We first examined whether ablation of FTase before exposure to DMBA had a benefit in tumor prevention. $FT^{lox/lox}$;$RERT^{ert/ert}$ mice (n = 20) were split into two cohorts and either left untreated or treated with 4OHT for 20 weeks to remove the FT *lox* allele. When these mice became 2 months old, both cohorts were exposed to a single dose of DMBA (25 μg/mouse) followed by repeated exposure to TPA for 12 additional weeks. As illustrated in Figure 7C, both cohorts of mice developed skin papillomas with similar incidence and kinetics regardless of the presence or absence of FTase. Genetic analysis of individual papillomas (n = 9) isolated from FT^{Δ};$RERT^{ert/ert}$ mice revealed that the FT *lox* alleles had been completely excised in these tumors (data not shown). To our surprise, H-*ras* oncogenes were present in both $FT^{lox/lox}$;$RERT^{ert/ert}$ and FT^{Δ};

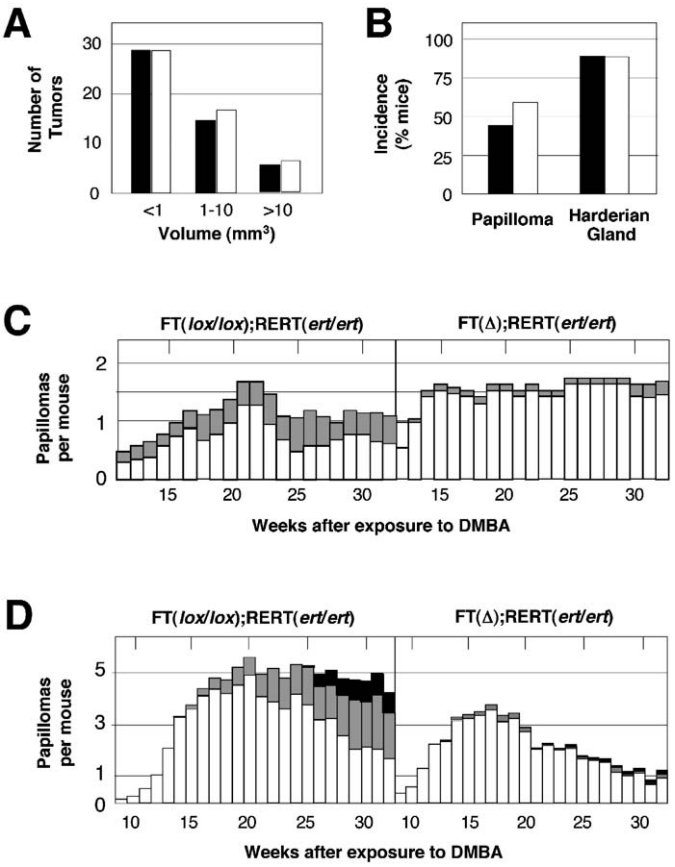

Figure 7. Effect of FTase ablation on tumor development

A: Number of adenomas and adenocarcinomas of the indicated sizes in lungs of 4OHT-treated $FT^{+/+}$;$K\text{-}ras^{+/V12}$;$RERT^{ert/ert}$ (filled columns) (n = 9) and FT^{Δ};$K\text{-}ras^{+/V12}$;$RERT^{ert/ert}$ (open columns) (n = 9) mice.

B: Percentage of mice described in **A** with papillomas and hyperplastic Harderian glands.

C: Number of papillomas in 2-month-old $FT^{lox/lox}$;$RERT^{ert/ert}$ (n = 10) and FT^{Δ};$RERT^{ert/ert}$ (n = 10) mice treated with a single dose of DMBA followed by treatment with TPA for 12 additional weeks. The average number of papillomas per mouse of less (open columns) or more (gray columns) than 4 mm of diameter is indicated.

D: Number of papillomas in $FT^{lox/lox}$;$RERT^{ert/ert}$ (n = 18) mice treated at P10 with a single dose of DMBA followed by treatment with TPA for 12 additional weeks. FT^{Δ};$RERT^{ert/ert}$ (n = 18) mice were generated by treatment of $FT^{lox/lox}$;$RERT^{ert/ert}$ animals with 4OHT 2 weeks after exposure to DMBA for the duration of the experiment (32 weeks). The average number of papillomas per mouse of less than 4 mm of diameter (open columns), between 4 and 8 mm of diameter (gray columns), and more than 8 mm of diameter (dark columns) is indicated.

RERT$^{ert/ert}$ mice with equal incidence (5 out of 9 and 6 out of 11 papillomas, respectively). All H-*ras* oncogenes were activated by the same CAA→CTA transversion in codon 61 (see the Supplemental Data available with this article online). We did not observe any significant differences in the size or pathological appearances between those tumors harboring H-*ras* oncogenes and those negative for this oncogene. These observations indicate that loss of the β subunit of FTase does not protect mice from skin tumor development, regardless of whether such tumors contain H-*ras* oncogenes or are induced by different mechanisms.

FTase ablation during tumor development

We also examined whether loss of FTase activity after tumor initiation had therapeutic benefit. Mice (n = 36) were either treated or not treated with 4OHT 2 weeks after the carcinogenic insult, a time when papillomas were still undetectable. At 15 weeks, both groups of mice had developed a similar number of papillomas (Figure 7D). However, at 20 to 25 weeks, *FT*$^{\Delta}$*;RERT*$^{ert/ert}$ mice displayed a significant reduction in the average number of papillomas per mouse (1.3 versus 4.7) and in tumor size (2.1 versus 4.7 mm of diameter) (Figure 7D). All papillomas (n = 10) examined from *FT*$^{\Delta}$*;RERT*$^{ert/ert}$ mice had lost their FT *lox* alleles and carried H-*ras* oncogenes activated by the same CAA→CTA transversion in codon 61 (see the Supplemental Data). As illustrated in Figure 8A, the levels of expression of H-Ras protein in these papillomas were increased by about 5- to 8-fold as compared with those present in normal skin. A similar increase in H-Ras expression was observed in papillomas derived from *FT*$^{\Delta}$*;RERT*$^{ert/ert}$ mice (Figure 8A).

Previous studies have indicated that the transforming activity of H-Ras oncoproteins requires their association with the plasma membrane, a process initiated by farnesylation of its carboxy-terminal CaaX motif (Downward, 2003; Sebti and Der, 2003). To examine whether H-Ras proteins were associated with membranous structures in tumors devoid of FTase, we fractionated cell extracts derived from *FT*$^{lox/lox}$*;RERT*$^{ert/ert}$ and *FT*$^{\Delta}$*;RERT*$^{ert/ert}$ papillomas. As depicted in Figure 8B, Western blot analysis revealed that at least half of the H-Ras protein expressed in papillomas lacking FTase was associated with the membranous P100 fraction (Figure 8B). As expected, the percentage of H-Ras protein present in the membrane fraction of control papillomas was close to 90% (Figure 8B). To determine whether the membrane localization of H-Ras in the absence of FTase is a unique property of papillomas or even a consequence of its oncogenic activation, we determined the subcellular localization of H-Ras in MEFs lacking FTase, a cell type in which H-Ras does not incorporate farnesyl residues (see Figures 4C and 4D). As shown in Figure 8C, the endogenous H-Ras protein expressed in *FT*$^{-/-}$*;RERT*$^{ert/ert}$ MEFs is also associated with membranous structures. Ectopic overexpression of H-Ras in these cells results in the presence of a limited percentage of the total H-Ras protein in the soluble fraction, a property also observed in control *FT*$^{lox/lox}$*;RERT*$^{ert/ert}$ MEFs (Figure 8C). These observations challenge the widely held concept that farnesylation is required for the association of H-Ras with membranes and for malignant transformation, at least in skin tumors.

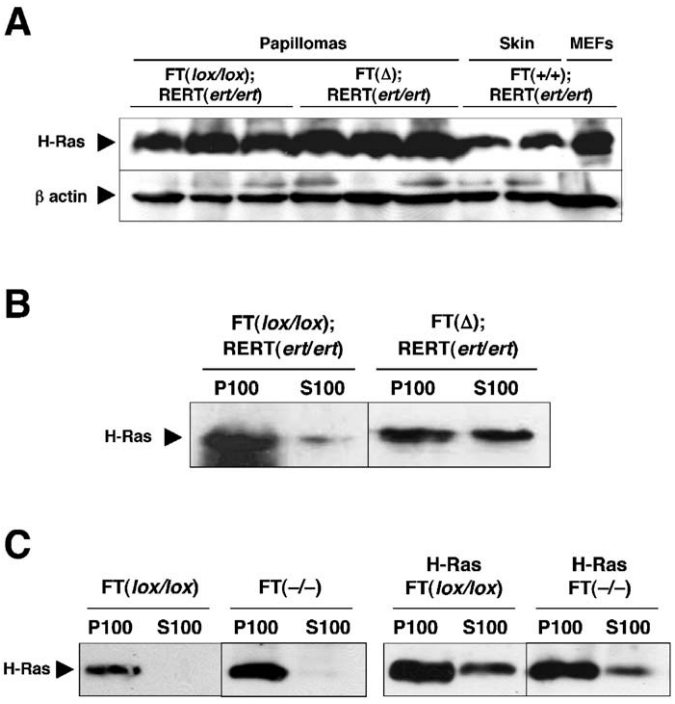

Figure 8. Expression levels and subcellular localization of H-Ras in tumor and normal cells lacking FTase

A: Western blot analysis of H-Ras in papillomas derived from *FT*$^{lox/lox}$*;RERT*$^{ert/ert}$ and *FT*$^{\Delta}$*;RERT*$^{ert/ert}$ mice. Skin tissue obtained from *FT*$^{+/+}$*;RERT*$^{ert/ert}$ mice treated with 4OHT and *FT*$^{+/+}$*;RERT*$^{ert/ert}$ MEFs were used as a reference. β actin was used as loading control.

B: Subcellular localization of H-Ras in papillomas. Total protein extracts from *FT*$^{lox/lox}$*;RERT*$^{ert/ert}$ and *FT*$^{\Delta}$*;RERT*$^{ert/ert}$ papillomas were fractionated into membranous (P100) and cytosolic (S100) fractions. H-Ras immunoprecipitates were fractionated in SDS gels and identified by Western blot analysis with antibodies specific for H-Ras.

C: Subcellular localization of H-Ras in fibroblasts null for FTase. Lysates from untransfected *FT*$^{lox/lox}$*;RERT*$^{ert/ert}$ and *FT*$^{-/-}$*;RERT*$^{ert/ert}$ MEFs (left) and from the same MEFs transfected with a plasmid containing the H-*ras* gene (right) were fractionated into membranous (P100) and cytosolic (S100) fractions and analyzed as described above. H-Ras *FT*$^{lox/lox}$*;RERT*$^{ert/ert}$ and H-Ras *FT*$^{-/-}$*;RERT*$^{ert/ert}$ cells express high levels of H-Ras (5- to 10-fold higher than untransfected MEFs). Migration of H-Ras is indicated by arrowheads. All MEFs are homozygous for the *ert* allele.

Discussion

Available evidence indicates that eukaryotic genomes, from yeast to humans, encode a single FTase made up of a specific catalytic subunit (β subunit) and a regulatory subunit (α subunit) shared with GGTase I. In agreement with these observations, ablation of the third exon of the gene encoding its β subunit results in complete loss of FTase activity, as determined by using three different substrates including H-Ras. In yeast, FTase-deficient cells are viable but display significant growth defects (Powers et al., 1986). The viability of these cells has been attributed to compensatory mechanisms involving cross-prenylation by GGTase I (Trueblood et al., 1993). FTase-deficient MEFs proliferate well, but their growth rate is significantly slower than that of wild-type cells. Moreover, quiescent FTase null MEFs do not reenter the cell cycle upon mitogenic stimuli as efficiently as their normal counterparts, suggesting a signal-

ing defect possibly involving inefficient activation of Ras proteins. However, it is also possible that lack of farnesylation of certain cell cycle proteins, such as the CENP kinetochore proteins, may contribute to this phenotype. FTase-deficient MEFs have a flat polygonal appearance and fail to grow as dense cultures. Moreover, their motility in standard in vitro wound assays is compromised, suggesting cytoskeletal defects (Zhang and Casey, 1996; Prendergast, 2001).

In vivo, FTase null embryos proliferate well and are able to implant in the maternal uterus. However, they undergo massive apoptosis a few hours after implantation. In vitro, FTase-deficient blastocysts (E3.5) appear normal and proliferate well up to 5–6 days after fertilization. However, they cease proliferation thereafter, indicating that the strict requirement for FTase is a cell autologous property. These observations could be explained by the absolute requirement of yet unidentified substrate(s) to undergo farnesylation during or immediately after implantation. However, it is also possible that farnesylation may be essential for even earlier stages of embryonic cell proliferation, but such requirement is provided by the maternal enzyme. In either case, our results establish that FTase activity is essential for cell proliferation during early embryogenesis (at least after E5.5) and that such requirement cannot be compensated by crossprenylation by either GGTase I or other protein isoprenyltransferases.

Protein farnesylation, however, is not essential for postnatal development. Young animals lacking FTase in most of their tissues develop normally to adulthood. Remarkably, *FT$^{\Delta}$; RERT$^{ert/ert}$* male mice efficiently transmit their FT null allele to their offspring, demonstrating that FTase activity is not essential for meiotic cell division, at least in males. Likewise, liver tissue regenerates in the absence of protein farnesylation after severe (70%) hepatectomy, regardless of the presence or absence of FTase activity. Young FTase-defective mice also recovered normally from other stress conditions, such as skin wounds and severe bleeding. Thus, unlike MEFs, postnatal fibroblasts respond normally to mitogenic stimuli. Likewise, hematopoiesis does not appear to be affected by lack of protein farnesylation in these young mice. These results suggest that protein farnesylation may not be required after birth. Alternatively, farnesylated proteins may undergo crossprenylation in postnatal tissues more efficiently than in embryonic cells.

FTase is required for proper responses to stress conditions in adult mice. Six-month-old FTase-deficient mice have delayed wound healing response (30% longer than wild-type animals). These mutant mice also display delayed maturation of erythroid precursor cells, as determined by a significant increase of proliferating progenitors in their spleens. This defect became more pronounced during response to severe bleeding. However, we did not observe significant defects in their bone marrow, suggesting that lack of FTase affects proliferation of committed erythroid precursors but not of pluripotent stem cells.

Protein farnesylation is the first step of a complex posttranslational process required for proper biological activity of CaaX-containing proteins (Zhang and Casey, 1996). Farnesylated proteins are recognized by specific endopeptidases that remove the carboxy-terminal aaX tripeptide (Boyartchuk et al., 1997). In *S. cerevisiae*, this process is carried out by two independent zinc endopeptidases, Rce1 and Afc1 (Boyartchuk et al., 1997). The mammalian homolog of the yeast *RCE1* gene has been recently isolated (Otto et al., 1999). Ablation of *rce1* in mice results in either late embryonic or early postnatal lethality (Kim et al., 1999). The longer survival of *rce1* null embryos compared to those lacking FTase is likely to be due to substrate proteins retaining partial function, since they can be isoprenylated even though postprenylation processing is abolished. *rce1* null MEFs also displayed retarded growth, at least partially due to the compromised association of Ras proteins with cellular membranes (Bergo et al., 2002).

Removal of the aaX sequence exposes the α-carboxyl group of the farnesylcysteine residue to a specific isoprenylcysteine methyltransferase (ICMT). ICMT was first identified in *S. cerevisiae* as the product of STE14, a gene necessary for the production of the a mating factor, but not for cell survival (Hrycyna et al., 1991). A related gene, *ICMT*, has been recently identified in human cells and shown to be functionally equivalent (Dai et al., 1998). Mice lacking Icmt die at about E10.5 (Bergo et al., 2001), a stage considerable later than that at which mice lacking FTase die. Icmt-defective fibroblasts grow more slowly than wild-type cells and are significantly resistant to transformation by K-*ras* oncogenes (Bergo et al., 2004). Interestingly, this property may not be a direct consequence of loss of activity of K-Ras but rather due to increased expression of the cell cycle inhibitor p21^{Cip1}, since K-*ras* oncogenes can efficiently transform Icmt-defective MEFs lacking p21^{Cip1} (Bergo et al., 2004). Moreover, *Icmt* null MEFs are also resistant to an oncogenic version of B-Raf, a nonprenylated protein that acts downstream of K-Ras (Bergo et al., 2004).

Much of the interest in protein farnesylation stemmed from the hypothesis that this posttranslational modification may be essential for the transforming activity of Ras oncoproteins (Zhang and Casey, 1996). The limited success of FTIs in early clinical trials has dampened some of this enthusiasm (Downward, 2003; Sebti and Der, 2003). These observations might be due, at least in part, to the fact that K-Ras4B, the Ras isoform most frequently mutated in human cancer, can undergo crossprenylation by GGTase I and thus could be insensitive to FTase inhibition (Lerner et al., 1997; Rowell et al., 1997; Whyte et al., 1997). Loss of FTase activity in lung adenomas induced by activation of an endogenous K-*ras* oncogene (Guerra et al., 2003) had no effect on either tumor incidence or tumor development. Whether these observations are due to alternative geranylgeranylation as suggested by the in vitro studies or to a different mechanism remains to be elucidated.

Unlike K-Ras, H-Ras proteins can only be isoprenylated by FTase. Loss of FTase activity by postnatal ablation of the gene encoding the catalytic β subunit had no significant effect on skin tumor formation (papillomas) in the DMBA + TPA protocol, a tumor model known to involve the reproducible activation of H-*ras* oncogenes (Balmain and Pragnell, 1983). Surprisingly, about two-thirds of these FTase-negative papillomas harbored H-*ras* oncogenes, the same percentage observed in *FT$^{lox/lox}$; RERT$^{ert/ert}$* control mice. These observations indicate that, in a physiological environment, H-*ras* oncogenes contribute to tumor development in the absence of FTase activity.

Removal of FTase after initiation of tumorigenesis had a significant effect on tumor progression as both the number of papillomas per animal and their average size were significantly reduced. Interestingly, those papillomas resistant to FTase ablation still carried H-*ras* oncogenes and retained the same levels of H-Ras expression as control tumors expressing the enzyme. Most surprisingly, a significant fraction of the H-Ras

protein present in these FTase null tumors was associated with membranous structures. Previous studies had conclusively demonstrated that replacement of the cysteine residue of the CaaX motif by serine, a mutation that prevents farnesylation of the H-Ras oncoprotein (Casey et al., 1989; Hancock et al., 1989), abolished the transforming activity of retroviral v-H-*ras* oncogenes in culture (Willumsen et al., 1984a; Willumsen et al., 1984b). These and other related observations have led to the widely held concept that nonfarnesylated H-Ras oncoproteins had no transforming activity, since they could not be properly localized in the plasma membrane. However, our results indicate that H-Ras oncoproteins expressed in cells devoid of FTase activity, and therefore presumed to be nonfarnesylated (see Figure 4), can associate with membranous structures and retain transforming activity, at least in DMBA-induced skin tumors. These observations make it necessary to reexamine the requirements for the association of H-Ras proteins with cellular membranes. We hypothesize that nonfarnesylated H-Ras proteins may interact with membranes in the absence of farnesylation through the palmitoyl residues attached to cysteines in positions 181 and 184. This posttranslational modification might be compromised in mutant H-Ras proteins in which cysteine 186, the target for farnesylation, has been replaced by serine. Elucidation of the posttranslational modifications of H-Ras proteins in FTase-defective cells by direct chemical analysis should help to establish the minimal requirements for their association with membranous structures and for transforming activity.

In summary, our observations illustrate that FTase is dispensable for tumor development induced by an endogenous K-*ras* oncogene, the *ras* oncogene most frequently activated in cancer patients. FTase is also dispensable for initiation of benign skin papillomas driven by H-*ras* oncogenes. However, removal of FTase after tumor initiation provides limited therapeutic benefit by decreasing the rate of tumor progression. Whether loss of FTase has more pronounced activity in other experimental tumor systems remains to be determined. Use of genetic approaches such as those described here should help to define those targets essential for tumor development.

Experimental procedures

Gene targeting and genotyping strategies

We have targeted the catalytic β subunit of FTase in ES cells by a strategy consisting in inserting three *loxP* sites flanking exon 3 and a PGK-*neo* cassette (*loxneo* allele) (Figure 1A). Detailed information regarding the generation of the targeting vector as well as the PCR strategy to identify wild-type, conditional (*lox*), and null (–) alleles can be found in the Supplemental Data.

Histology and cell culture assays

E7.5 deciduas or adult tissues were surgically removed, fixed in 10% buffered formalin, and embedded in paraffin using standard procedures. Sections (6 μm) were stained with hematoxylin and eosin (H&E). TUNEL assays were performed using the in situ cell death detection kit (Roche). Cell proliferation was determined by immunostaining with anti-Ki67 antibodies (Biotechnologies). Blastocysts (E3.5) were collected by uterine flush with M2 medium (Sigma) and individually cultured on gelatin-coated 96-well plates. For BrdU labeling, blastocysts were incubated for 2 hr with 10 μM BrdU. BrdU-positive cells were detected with BrdU detection kit I (Roche) according to the manufacturer's instructions. MEFs were isolated from $FT^{lox/lox}$; $RERT^{ert/ert}$ E13.5 embryos and cultured in Dulbecco's modified Eagle's medium (DMEM) supplemented with 2 mM glutamine, 1% penicillin/streptomycin and 10% calf serum as described (Malumbres et al., 2004) in the absence or presence of 4OHT. Proliferation and S phase entry assays were also carried out as previously described (Malumbres et al., 2004). For in vitro motility assays, confluent monolayers were subjected to mechanical injury with an adaptor scraper, and images were recorded every 10 min for the required amount of time with a confocal microscope (Leica SP2).

Animal treatments

Mice were injected intraperitoneally three times a week with 0.5 mg of oil-homogenized 4OHT (Sigma). Two-month-old mice were hepatectomized as previously described (Higgins and Anderson, 1931). Two hours before sacrifice, mice were injected with 60 μg of BrdU/g of body weight to analyze cell proliferation. For wound healing experiments, mice (2 and 6 month old) were anesthetized, their backs were shaved, and a circular full-thickness wound (6 mm in diameter) was created by excision of the skin with curved scissors. For bleeding experiments, 0.8 ml of blood was taken from the eye of 2- and 6-month-old animals. Before bleeding, an analgesic was administrated. For carcinogenesis experiments, mice were treated with a single dose of DMBA (Sigma) (25 μg for 10-week-old mice and 0.5 mg for P10 mice) followed by exposure to TPA (Sigma) (12.5 μg twice weekly) for a total of 12 weeks.

Flow cytometry

Cells obtained from spleen and bone marrow were washed, resuspended in PBS, and incubated with PharM Lyse (Pharmigen). Cell surface markers used to identify hematopoietic cell populations included CD3, CD4, CD8, CD11b, CD45, CD16/CD32, B220, GR1, IL-7aR, Pan-NK (DX-5), and Ter119 (Pharmigen). Cell populations were quantified using a BD Biosciences (FACScan). In each case, 20,000 events were collected.

Subcellular fractionation and Western blot analysis

Membrane (P100) and cytosolic (S100) fractions were isolated according to established protocols (Bergo et al., 2002). H-Ras was immunoprecipitated from 1 mg of P100 and S100 fractions with specific antibodies (Ab-1; Oncogene Research Products). Western blots were performed using different H-Ras-specific antibodies (C20; Santa Cruz Biotechnology), or antibodies against HDJ2 (MDJ2-human homolog, KA2A5.6; NeoMarkers) and β-actin (AC-15; Sigma). Antibodies were detected with the appropriate horseradish peroxidase-linked secondary antibody and visualized with an enhanced chemiluminescent (ECL) system (Amersham).

FTase activity assays

FTase and/or GGTase I activities were measured either using the [^{3}H] SPA enzyme assay kit (Amersham) or by measuring incorporation of [^{3}H]-FPP or [^{3}H]-GGPP into a recombinant H-Ras protein by cytosolic fractions prepared from MEFs as previously described (Fiordalisi et al., 2003). For the incorporation of [^{3}H]-FPP on the endogenous H-Ras protein, we incubated 1 mg of total protein extract in 1 ml of assay buffer ([^{3}H] SPA enzyme assay kit; Amersham) containing 12 μM [^{3}H]-FPP (12 Ci/mmol; Amersham). H-Ras was immunoprecipitated as described above, resolved on 12% SDS-PAGE gels, and exposed to film.

Supplemental data

The Supplemental Data include Supplemental Experimental Procedures and one supplemental figure and can be found with this article online at http://www.cancercell.org/cgi/content/full/7/4/313/DC1/.

Acknowledgments

We thank Rut González, Marta San Román, and Raquel Villar for excellent technical assistance; Carmen Gómez, Marta Riffo, and Sagrario Ortega for their help with the generation of gene-targeted mice; Ignacio Segovia for his help with animal husbandry; Arantxa García, Diego Mejías, and María Montoya for their help with FACS analysis; and Lucía Pérez-Gallego for helpful discussions. The early phases of this work were carried out at the Centro Nacional de Biotecnología (CSIC; Madrid). We are indebted to M. Esteban and the Faculty for making their facilities available to us. This work was supported by grants from the V Framework Programme of the European Union (QLK3-1999-00875) to M.B. and from the Ministerio de Ciencia y Tecnologia (SAF2001-0058) and Fondo de Investigación Sanitaria (00/

0109) to J.V. P.D. was supported by the Association pour la Recherche contre le Cancer (ARC). P.J.C. was supported by NIH grant GM46372. N.M. was supported by a BEFI Fellowship from the Fondo de Investigación Sanitaria. The CNIO is partially supported by the RTICCC (Red de Centros de Cáncer; FIS C03/10).

Received: October 12, 2004
Revised: December 1, 2004
Accepted: March 2, 2005
Published: April 18, 2005

References

Armstrong, S.A., Hannah, V.C., Goldstein, J.L., and Brown, M.S. (1995). CAAX geranylgeranyl transferase transfers farnesyl as efficiently as geranylgeranyl to RhoB. J. Biol. Chem. *270*, 7864–7868.

Balmain, A., and Pragnell, I.B. (1983). Mouse skin carcinomas induced in vivo by chemical carcinogens have a transforming Harvey-ras oncogene. Nature *303*, 72–74.

Bergo, M.O., Leung, G.K., Ambroziak, P., Otto, J.C., Casey, P.J., Gomes, A.Q., Seabra, M.C., and Young, S.G. (2001). Isoprenylcysteine carboxyl methyltransferase deficiency in mice. J. Biol. Chem. *276*, 5841–5845.

Bergo, M.O., Ambroziak, P., Gregory, C., George, A., Otto, J.C., Kim, E., Nagase, H., Casey, P.J., Balmain, A., and Young, S.G. (2002). Absence of the CAAX endoprotease Rce1: effects on cell growth and transformation. Mol. Cell. Biol. *22*, 171–181.

Bergo, M.O., Gavino, B.J., Hong, C., Beigneux, A.P., McMahon, M., Casey, P.J., and Young, S.G. (2004). Inactivation of Icmt inhibits transformation by oncogenic K-Ras and B-Raf. J. Clin. Invest. *113*, 539–550.

Boyartchuk, V.L., Ashby, M.N., and Rine, J. (1997). Modulation of Ras and a-factor function by carboxyl-terminal proteolysis. Science *275*, 1796–1800.

Brocard, J., Warot, X., Wendling, O., Messaddeq, N., Vonesch, J.L., Chambon, P., and Metzger, D. (1997). Spatio-temporally controlled site-specific somatic mutagenesis in the mouse. Proc. Natl. Acad. Sci. USA *94*, 14559–14563.

Casey, P.J., Solski, P.A., Der, C.J., and Buss, J.E. (1989). p21ras is modified by a farnesyl isoprenoid. Proc. Natl. Acad. Sci. USA *86*, 8323–8327.

Dai, Q., Choy, E., Chium, V., Romano, J., Slivka, S.R., Steitz, S.A., Michaelis, S., and Philips, M.R. (1998). Mammalian prenylcysteine carboxl methyltransferase is in the endoplasmic reticulum. J. Biol. Chem. *273*, 15030–15034.

Davis, A.R., Alevy, Y.G., Chellaiah, A., Quinn, M.T., and Mohanakumar, T. (1998). Characterization of HDJ-2, a human 40 kD heat shock protein. Int. J. Biochem. Cell Biol. *30*, 1203–1221.

Downward, J. (2003). Targeting RAS signalling pathways in cancer therapy. Nat. Rev. Cancer *3*, 11–22.

Du, W., Lebowitz, P.F., and Prendergast, G.C. (1999). Cell growth inhibition by farnesyltrasnferase inhibitors is mediated by gain of geranylgeranylated RhoB. Mol. Cell. Biol. *19*, 1831–1840.

Fiordalisi, J.J., Johnson, R.L., II, Weinbaum, C.A., Sakabe, K., Chen, Z., Casey, P.J., and Cox, A.D. (2003). High affinity for farnesyltransferase and alternative prenylation contribute individually to K-Ras4B resistance to farnesyltransferase inhibitors. J. Biol. Chem. *278*, 41718–41727.

Gibbs, J.B., Oliff, A., and Kohl, N.E. (1994). Farnesyltransferase inhibitors: Ras research yields a potential cancer therapeutic. Cell *77*, 175–178.

Glomset, J.A., Gelb, M.H., and Farnsworth, C.C. (1990). Prenyl proteins in eukaryotic cells: a new type of membrane anchor. Trends Biochem. Sci. *15*, 139–142.

Guerra, C., Mijimolle, N., Dhawahir, A., Dubus, P., Barradas, M., Serrano, M., Campuzano, V., and Barbacid, M. (2003). Tumor induction by an endogenous K-ras oncogene is highly dependent on cellular context. Cancer Cell *4*, 111–120.

Hancock, J.F., Magee, A.I., Childs, J.E., and Marshall, C.J. (1989). All Ras proteins are polyisoprenylated but only some are palmitoylated. Cell *57*, 1167–1177.

Higgins, G.M., and Anderson, R.M. (1931). Restoration of the liver of the white rat following partial surgical removal. Arch. Pathol. *12*, 186–202.

Hrycyna, C.A., Sappertein, S.K., Clarke, S., and Michaeli, S. (1991). The Saccharomyces cerevisiae STE14 gene encodes a methyltransferase that mediates C-terminal methylation of a-factor and RAS proteins. EMBO J. *10*, 1699–1709.

James, G.L., Goldstein, J.L., and Brown, M.S. (1995). Polylysine and CVIM sequences of K-RasB dictate specificity of prenylation and confer resistance to benzodiazepine peptidomimetic in vitro. J. Biol. Chem. *270*, 6221–6226.

Kim, E., Ambroziak, P., Otto, J.C., Taylor, B., Ashaby, M., Shannon, K., Casey, P.J., and Young, S.G. (1999). Disruption of the mouse Rce1 gene results in defective Ras processing and mislocalization of Ras within cells. J. Biol. Chem. *274*, 8383–8390.

Kohl, N.E., Wilson, F.R., Mosser, S.D., Giuliani, E., deSolms, S.J., Conner, M.W., Anthony, N.J., Holtz, W.J., Gomez, R.P., Lee, T.J., et al. (1994). Protein farnesyltransferase inhibitors block the growth of ras-dependent tumors in nude mice. Proc. Natl. Acad. Sci. USA *91*, 9141–9145.

Kohl, N.E., Omer, C.A., Conner, M.W., Anthony, N.J., Davide, J.P., deSolms, S.J., Giuliani, E.A., Gomez, R.P., Graham, S.L., Hamilton, K., et al. (1995). Inhibition of farnesyltransferase induces regression of mammary and salivary carcinomas in ras transgenic mice. Nat. Med. *1*, 792–797.

Lebowitz, P.F., Davide, J.P., and Predergast, G.C. (1995). Evidence that farnesyltransferase inhibitors suppress Ras transformation by interfering with Rho activity. Mol. Cell. Biol. *15*, 6613–6622.

Lerner, E.C., Zhang, T.T., Knowles, D.B., Qian, Y., Hamilton, A.D., and Sebti, S.M. (1997). Inhibition of the prenylation of K-Ras, but not H- or N-Ras, is highly resistant to CAAX peptidomimetics and requires both a farnesyltransferase and a geranylgeranyltransferase I inhibitor in human tumor cell lines. Oncogene *15*, 1283–1288.

Malumbres, M., Sotillo, R., Santamaría, D., Galán, J., Cerezo, A., Ortega, S., Dubus, P., and Barbacid, M. (2004). Mammalian cells cycle without the D-type cyclin-dependent kinases Cdk4 and Cdk6. Cell *118*, 493–504.

Otto, J.C., Kim, E., Young, S.G., and Casey, P.J. (1999). Cloning and characterization of mammalian prenyl protein-specific portease. J. Biol. Chem. *274*, 8379–8382.

Powers, S., Michaelis, S., Broek, D., Santa Anna, S., Field, J., Hereskowitz, I., and Wigler, M. (1986). RAM, a gene of yeast required for a functional modification of RAS proteins and for production of mating pheromone a-factor. Cell *47*, 413–422.

Prendergast, G.C. (2001). Actin' up: RhoB in cancer and apoptosis. Nat. Rev. Cancer *1*, 162–168.

Reid, T.S., Terry, K.L., Casey, P.J., and Beese, L.S (2004). Crystallographic analysis of CaaX prenyltransferases complexed with substrates defines rules of protein substrate selectivity. J. Mol. Biol. *343*, 417–433.

Rowell, C.A., Kowalczyk, J.J., Lewis, M.D., and Garcia, A.M. (1997). Direct demonstration of geranylgeranylation and farnesylation of Ki-Ras in vivo. J. Biol. Chem. *272*, 14093–14097.

Schwenk, F., Baron, U., and Rajewsky, K. (1995). A cre-transgenic mouse strain for the ubiquitous deletion of loxP-flanked gene segments including deletion in germ cells. Nucleic Acids Res. *23*, 5080–5081.

Seabra, M.C., Mules, E.H., and Hume, A.N. (2002). Rab GTPases, intracellular traffic and disease. Trends Mol. Med. *8*, 23–30.

Sebti, S.M., and Der, C.J. (2003). Opinion: Searching for the elusive targets of farnesyltransferase inhibitors. Nat. Rev. Cancer *3*, 945–951.

Trueblood, C.E., Ohya, Y., and Rine, J. (1993). Genetic evidence for in vivo cross specificity of the CaaX-box protein prenyltransferases farnesyltransferase and geranylgeranyltransferase-I in Saccharomyces cerevisiae. Mol. Cell. Biol. *13*, 4260–4275.

Whyte, D.B., Kirschmeier, P., Hockenberry, T.N., Nuñez-Oliva, I., James, L.,

Catino, J.J., Bishop, W.R., and Pai, J.K. (1997). K- and N-Ras are geranylgeranylated in cells treated with farnesyl protein transferase inhibitors. J. Biol. Chem. *272*, 14459–14464.

Willumsen, B.M., Christensen, A., Hubbert, N.L., Papageorge, A.G., and Lowy, D.R. (1984a). The p21 ras C-terminus is required for transformation and membrane association. Nature *310*, 583–586.

Willumsen, B.M., Norris, K., Papageorge, A.G., Hubbert, N.L., and Lowy, D.R. (1984b). Harvey murine sarcoma virus p 21 ras protein: biological and biochemical significance of the cysteine nearest the carboxy terminus. EMBO J. *3*, 2581–2585.

Zhang, F.L., and Casey, P.J. (1996). Protein prenylation: molecular mechanisms and functional consequences. Annu. Rev. Biochem. *65*, 241–269.